STATISTICAL SELF-CALIBRATION OF SPOT SATELLITE IMAGING INSTRUMENT

H. CARFANTAN
Laboratoire d'Astrophysique de l'Observatoire Midi-Pyrénées,
14 Av. É. Belin, 31400 Toulouse, France[§]

J. IDIER
Laboratoire des Signaux et Systèmes
SUPÉLEC, *Plateau de Moulon, 91192 Gif–sur–Yvette Cedex, France*[¶]

AND

B. BEGHIN, A. MEYGRET AND B. ROUGE
Centre National d'Études Spatiales,
18 Av. É. Belin, 31400 Toulouse, France[‖]

Abstract. SPOT satellites imaging instruments acquire rows of up to 6000 elements using a CCD linear array. The other dimension is obtained by the column-wise scanning resulting from the motion of the satellite. In practice, the responses of the detectors are not strictly identical along the array, which generates a stripe effect in the direction of columns. Our aim is to perform the calibration of the detectors response from the observed image, without supervision, in the restricted case of perfectly linear responses.

In a Bayesian framework, we rely on a first-order Markov model for the image and on a Gaussian model for the gains of the detector. The MAP estimate minimizes a criterion, quadratic, convex, or non convex according to the chosen Markov model.

In the quadratic case, MAP computation amounts to solving a tridiagonal linear system. In the other cases, we take advantage of introducing an equivalent augmented *half-quadratic* criterion, which can be minimized by iterately solving tridiagonal linear systems. Minimizing non convex criteria provides the best results, although convergence towards the global minimizer is not ensured in this case.

Key words: MAP estimation of detectors gain, edge-preserving Markov model, augmented half-quadratic criterion

[§]Email: Herve.Carfantan@obs-mip.fr
[¶]Email: Jerome.Idier@lss.supelec.fr
[‖]Email: Benoit.Beghin@cnes.fr,Aime.Meygret@cnes.fr,Bernard.Rouge@cnes.fr

1. Problem Statement

1.1. IMAGE FORMATION

SPOT (*Satellites Pour l'Observation de la Terre*, earth observations satellites) imaging instruments are designed to acquire complete rows of 3000 pixels in multispectral mode and 6000 in panchromatic mode, using a CCD linear array. The other dimension is obtained by the column-wise scanning that results from the motion of the satellite along its orbit (see Figure 1). In practice, the response of the detectors are not strictly identical along the array, which generates a stripe effect in the direction of columns that must be compensated for.

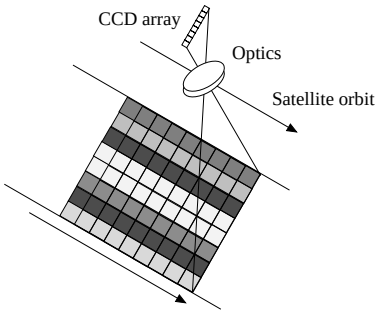

Figure 1. Image formation of SPOT satellite instrument.

1.2. DETECTORS MODEL

As a first approximation, the detectors response can be considered linear. Perfect detectors having an identity response, imperfections then correspond to unknown gains $g_c > 0$, one for each column of pixels. The relation between the perfect data (data from perfect detectors) $\boldsymbol{x} = \{x_{r,c}\}_{r=1..R,c=1..C}$ (row r, column c) and actual data $\boldsymbol{y} = \{y_{rc}\}_{r=1..R,c=1..C}$ can thus be written:

$$y_{rc} = g_c x_{r,c} \tag{1}$$

which is a multiplicative relation. An equivalent relation can be written using the logarithm of (1): $\log y_{rc} = \log g_c + \log x_{r,c}$. For simplicity, we will note hereafter $\boldsymbol{y}^l = \{y^l_{rc}\} = \{\log y_{rc}\}$, $\boldsymbol{x}^l = \{x^l_{r,c}\} = \{\log x_{r,c}\}$ and $\boldsymbol{g}^l = \{g^l_c\} = \{\log g_c\}$ which leads to the additive relation:

$$y^l_{rc} = g^l_c + x^l_{r,c}. \tag{2}$$

1.3. CALIBRATION

At the present time, identification of the gain of the detectors is performed during calibration phase. During these phases, the satellites imaging instruments observe a landscape that is as uniform as possible, such as the poles. In such experimental conditions, even a simple empirical estimator (as will be presented in § 2.1) can give satisfactory estimated gains. Such a calibration system is used periodically to check and, if necessary, adjust the detectors response.

The objective is to estimate the gains $\boldsymbol{g} = \{g_c\}_{c=1..C}$ from any SPOT image (typically, of $R = 6000$ rows and $C = 6000$ columns). Since the perfect data $x_{r,c}$ are unknown, such a problem is heavily indeterminate. On the other hand, we can rely on statistical redundancy, since only C unknown gains have to be estimated from $R \times C$ measured pixels. The simplest approaches are based on empirical statistics (§ 2.1), whereas our contribution explicitly introduces a model for the true scene $\boldsymbol{x}$, so that it can be integrated out of the problem to define and maximize a likelihood function (§ 2.2 and § 2.3).

2. Gain estimation

2.1. EMPIRICAL ESTIMATES

From an empirical viewpoint, we can define estimates that converge towards the true gains for an infinite number of acquired rows, in an ergodic stationary statistical framework. In such a framework, the empirical mean of a column $\frac{1}{R}\sum_{r=1}^{R} y_{rc} = g_c \frac{1}{R}\sum_{r=1}^{R} x_{r,c}$ is assumed to converge towards $g_c m_x$, where $m_x = \mathrm{E}[X_{r,c}]$ is the mean of the perfect data, while the empirical mean of the whole image $\frac{1}{RC}\sum_{r=1}^{R}\sum_{c=1}^{C} y_{rc}$ converges towards $m_x \mathrm{E}[g_c] = m_x$ (if we assume $\mathrm{E}[g_c] = 1$). Then one can define

$$\widehat{g}_c^0 = \frac{C \sum_{r=1}^{R} y_{rc}}{\sum_{c'=1}^{C}\sum_{r=1}^{R} y_{r,c'}},$$

which is expected to converge towards g_c.

However, as will be seen in § 4.2, such an estimator is very sensitive to the observed landscape for a limited number of rows. A more robust version can be defined, in which the mean of the image is computed locally w.r.t. columns, using a window $\{w_k\}_{k=-L..L}$. For columns $c = L+1, \ldots, C-L$, let

$$\widehat{g}_c^1 = \frac{(2L+1)\sum_{r=1}^{R} y_{rc}}{\sum_{c'=c-L}^{c+L}\left(w_{c'-c}\sum_{r=1}^{R} y_{r,c'}\right)}.$$

2.2. MAXIMUM LIKELIHOOD ESTIMATOR

If a probabilistic law with a density p_X is chosen for $\boldsymbol{x}$, then a likelihood $L(\boldsymbol{g}\,;\boldsymbol{y}) = p_Y(\boldsymbol{y}\,;\boldsymbol{g})$ can be defined. Considering the multiplicative relation (1) as a change

of variables between random vectors $\boldsymbol{X}$ and $\boldsymbol{Y}$, we have

$$p_Y(\boldsymbol{y}\,;\boldsymbol{g}) = \frac{1}{\prod_{c=1}^{C} g_c^R} p_X(\tilde{\boldsymbol{x}}), \quad \text{with } \tilde{\boldsymbol{x}} = \{\tilde{x}_{r,c}\} \quad \text{and } \tilde{x}_{r,c} = \frac{y_{rc}}{g_c}. \tag{3}$$

The additive relation (2) expresses an even simpler change of variables between $\boldsymbol{X}^l$ and $\boldsymbol{Y}^l$:

$$p_{Y^l}(\boldsymbol{y}^l\,;\boldsymbol{g}^l) = p_{X^l}(\tilde{\boldsymbol{x}}^l), \quad \text{with } \tilde{\boldsymbol{x}}^l = \{\tilde{x}^l_{r,c}\} \quad \text{and } \tilde{x}^l_{r,c} = y^l_{rc} - g^l_c.$$

2.2.1. *Model for the image*

In the following, we have adopted a basic Markovian structure for the image $\boldsymbol{X}$, which is widely used in the field of image restoration. The chosen model is a first-order Markov field, with pairwise interactions restricted to differences between neighboring pixels:

$$p_X(\boldsymbol{x}) = \exp\left\{-\frac{1}{T}\sum_{m\sim n}\phi(x_m - x_n)\right\} \tag{4}$$

where $m \sim n$ means summation over all distinct pairs $\{m, n\}$ of neighboring sites. Note that such a model is improper since $\int_{\boldsymbol{x}} p_X(\boldsymbol{x})\,d\boldsymbol{x} = +\infty$, but this happens to be of no practical consequence in the present context.

Classically, one chooses ϕ as an even function, non decreasing on $\mathbb{R}^+$, such as

$$\phi(x) = \begin{cases} x^2 & \text{quadratic} \\ |x| & L_1 \text{ norm} \\ \sqrt{s^2 + x^2} & \text{hyperbolic} \\ \frac{x^2}{s^2+x^2} & \text{non convex [1]} \end{cases} \tag{5}$$

Whereas the first two have a uniform behaviour over $\mathbb{R}$ (respectively, quadratic and linear), the other two behave quadratically near zero while they are asymptotically linear or constant, respectively. The change of behaviour roughly happens around the threshold parameter s, as seen on Figure 2.

For the logarithmic version $\boldsymbol{X}^l$, we have tested the same Markov model with the four possible definitions for ϕ.

2.2.2. *Likelihood criteria*

From the multiplicative relation (1), according to (3) and (4), the maximum likelihood (ML) estimate minimizes the criterion:

$$J_{ML}(\boldsymbol{g}) = \frac{1}{T}\sum_{r,c}\phi\left(\frac{y_{rc}}{g_c} - \frac{y_{r,c+1}}{g_{c+1}}\right) + \frac{1}{T}\sum_{r,c}\phi\left(\frac{y_{rc} - y_{r+1,c}}{g_c}\right) + R\sum_c \log(|g_c|). \tag{6}$$

The first and second terms correspond to horizontal and vertical neighbors, respectively, and the last term to the change of variable in the probability law (3).

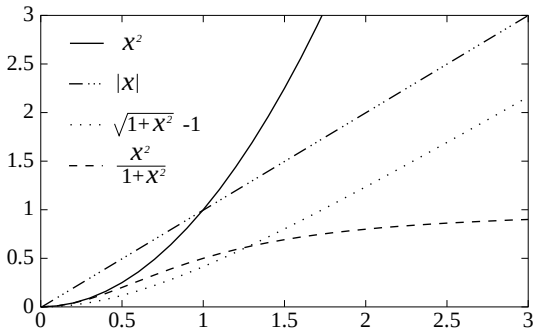

Figure 2. Four functions defined by (5). The last two are depicted for $s = 1$.

In the additive framework (2), similarly, the maximum likelihood estimate minimizes the criterion:

$$J^l_{ML}(\boldsymbol{g}^l) = \frac{1}{T}\sum_{r,c} \phi((g^l_c - y^l_{rc}) - (g^l_{c+1} - y^l_{r,c+1})) \tag{7}$$

in which only the terms corresponding to horizontal neighbors appear.

2.3. MAXIMUM *A POSTERIORI* ESTIMATE

Without additional information, the problem is still globally indeterminate, since couples $(\alpha\boldsymbol{g}, \frac{1}{\alpha}\boldsymbol{x})$ are equally likely for any $\alpha > 0$. In the additive framework, because the Markov model (4) is invariant through the global translation $\boldsymbol{x} \to \boldsymbol{x} - \log\alpha$, (7) is invariant through the transformation $\boldsymbol{g} \to \alpha\boldsymbol{g}$, $\alpha > 0$. In the multiplicative framework, the Markov model (4) is scale invariant up to a change of hyperparameter value (T, s), so that the indeterminacy is still present.

Modeling the gains as random variables of mean $\mathrm{E}[g_c] = 1$ provides an easy way of alleviating the indeterminacy, so we are naturally led to Bayesian estimation scheme. In particular, the maximum *a posteriori* (MAP) estimate maximizes the posterior law $p_{G|Y}$.

Considering an i.i.d. Gaussian law for the gains or for the log of the gains (of mean $\mathrm{E}[g^l_c] = 0$ in the latter case), the MAP estimate maximizes the criterion:

$$J_{MAP}(\boldsymbol{g}) = J_{ML}(\boldsymbol{g}) + \frac{1}{2\sigma_g^2}\sum_c (g_c - 1)^2 \tag{8}$$

in the case of the multiplicative relation, and:

$$J^l_{MAP}(\boldsymbol{g}^l) = J^l_{ML}(\boldsymbol{g}^l) + \frac{1}{2\sigma_g^2}\sum_c (g^l_c)^2 \tag{9}$$

in the additive counterpart. Both criteria can be seen as penalized versions of corresponding maximum likelihood criteria (6) and (7).

3. Optimization

3.1. SPECIAL CASE OF ML FOR THE ADDITIVE RELATION

The computation of the maximum likelihood estimate in the additive case (2) is particularly simple from the optimization viewpoint. Let us introduce $\delta g_c^l = g_c^l - g_{c+1}^l$. Then, criterion (7) reads

$$J_{ML}^l(\delta \boldsymbol{g}^l) = \sum_{r,c} \phi(\delta g_c^l - \delta y_{rc}^l),$$

with $\delta y_{rc}^l = \delta y_{rc}^l - \delta y_{r,c+1}^l$. Such a criterion is separable and each variable δg_c^l can be computed as the minimizer of

$$J_{ML}^l(\delta g_c^l) = \sum_{r} \phi(\delta g_c^l - \delta y_{rc}^l). \tag{10}$$

In the special case of a Gauss-Markov model for the image ((4) for $\phi(x) = x^2$), the ML estimate of δg_c^l can be computed explicitly as the empirical mean of δy_{rc}^l within column c. For $\phi(x) = |x|$, it can be computed as the median value of column c. For other choices of ϕ, a unidimensional search algorithm as to be implemented to compute the estimates.

3.2. QUADRATIC CASE $\phi(X) = X^2$

Minimization of a quadratic criterion amounts to solve a linear system. In the case of the additive relation (2), ML and MAP criteria (7), (9) are quadratic if we consider a Gauss-Markov model ($\phi(x) = x^2$) for the logarithm of the image.

Such a condition is not sufficient to grant linearity in the multiplicative case. Although attenuations $\boldsymbol{a} = \{a_c\}_{c=1..C}$, $a_c = 1/g_c$ intervene linearly as arguments of functions ϕ, the change of variable also introduces a logarithmic term in (6) or (8). Since the gains are known to be close to one, we can approximate $\log |a_c| \approx a_c - 1$ and $1/a_c \approx 2 - a_c$. This leads to the following expressions

$$J_{ML}(\boldsymbol{a}) = \frac{1}{T} \sum_{r,c} (a_c y_{rc} - a_{c+1} y_{r,c+1})^2 + \frac{1}{T} \sum_{r,c} a_c^2 (y_{rc} - y_{r+1,c})^2 - R \sum_c a_c, \tag{11}$$

$$J_{MAP}(\boldsymbol{a}) = J_{ML}(\boldsymbol{a}) + \frac{1}{2\sigma_g^2} \sum_c (a_c - 1)^2 . \tag{12}$$

Finally, the minimizers of (7), (9), (11) and (12) can be computed at a very low numerical cost as the corresponding linear systems are tridiagonal.

3.3. NON QUADRATIC CASES

The efficiency of non quadratic functions ϕ have been proved in the construction of edge-preserving models for image restoration [1,2]. Although the optimization is not as simple as in the quadratic case, one can take advantage of introducing

augmented half-quadratic criteria as proposed in [3,2,4]. Such criteria are quadratic functions of the main unknowns (*i.e.*, pixel intensities in image restoration), but they also integrate auxiliary variables, so that half-quadratic criteria are globally non quadratic. Following Geman and Reynolds [3], the construction of such criteria is based on the following duality theorem.

If ϕ is even, continuously differentiable and $\phi(\sqrt{\cdot})$ is concave on $\mathbb{R}_+$, $\exists\psi$ such that:

$$\phi(u) = \inf_b (bu^2 + \psi(b)) = \hat{b}u^2 + \psi(\hat{b})$$

where $\psi(b) = \sup_u (\phi(u) - bu^2)$ and

$$\hat{b} = \begin{cases} \lim_{u\to 0^+} \phi'(u)/2u & \text{if } u = 0, \\ \phi'(u)/2u & \text{otherwise.} \end{cases} \tag{13}$$

In the present context, the unknowns are not pixel intensities but gain or attenuation values. Half-quadratic criteria can be easily deduced from the ML (7) and MAP (9) criteria and also from the approximate ML (11) and MAP (12) criteria. The number of required auxiliary variables is $2(R-1)(C-1)$ for the multiplicative relation:

$$\begin{aligned} K_{ML}(\boldsymbol{a},\boldsymbol{b}) &= \frac{1}{T}\sum_{r,c}\left(b^{\mathrm{h}}_{rc}(a_c y_{rc} - a_{c+1}y_{r,c+1})^2 + \psi(b^{\mathrm{h}}_{rc})\right) \\ &\quad + \frac{1}{T}\sum_{r,c}\left(b^{\mathrm{v}}_{rc}(a_c(y_{rc} - y_{r+1,c}))^2 + \psi(b^{\mathrm{v}}_{rc})\right) - R\sum_c a_c, \\ K_{MAP}(\boldsymbol{a},\boldsymbol{b}) &= K_{ML}(\boldsymbol{a},\boldsymbol{b}) + \frac{1}{2\sigma_g^2}\sum_c (a_c - 1)^2, \end{aligned}$$

and only $(R-1)(C-1)$ for the additive relation:

$$\begin{aligned} K^l_{ML}(\boldsymbol{g}^l,\boldsymbol{b}) &= \frac{1}{T}\sum_{r,c} b_{rc}((g^l_c - y^l_{rc}) - (g^l_{c+1} - y^l_{r,c+1}))^2, \\ K^l_{MAP}(\boldsymbol{g}^l,\boldsymbol{b}) &= K^l_{ML}(\boldsymbol{g}^l,\boldsymbol{b}) + \frac{1}{2\sigma_g^2}\sum_c \left(g^l_c\right)^2. \end{aligned}$$

Minimization of such an augmented criterion can be performed by alternate descent on the original unknowns and on the auxiliary variables [2,4].

- Minimization with respect to the original variables $\boldsymbol{g}^l$ or $\boldsymbol{a}$ when $\boldsymbol{b}$ is held constant amounts to solve tridiagonal linear systems, akin to § 3.2.
- Minimization with respect to the auxiliary variables $\boldsymbol{b}$ when $\boldsymbol{g}^l$ or $\boldsymbol{a}$ are held constant can be performed separately for each b_{rc} and the solution is explicitly given by (13).

Moreover, in such an alternate minimization scheme, there is no need to store auxiliary variables $\boldsymbol{b}$, but only to update the tridiagonal system with their current values. Compared to classical descent algorithms, such algorithms are easy to implement since only a tridiagonal linear system is solved at each iteration, and no

line search is required. Still, convergence is guaranteed for the hyperbolic case and almost any other convex function ϕ [4]. In the case of non convex functions, the same procedure can still be used but it can be stuck in a local minimum [5]. In our context, convergence is reached in less than 20 iterations.

4. Simulations and results

4.1. IMAGES SIMULATIONS

To compare the different approaches we worked on simulated data, for which both perfect data $\{x_{r,c}\}$ and gains $\{g_c^*\}$ are known. We simulated the SPOT acquisition process from a photograph with a resolution of one meter (see Figure 3). We artificially placed a mirrored image next to the original one. The result is double width image of $C = 1814$ columns and $R = 2380$ rows.

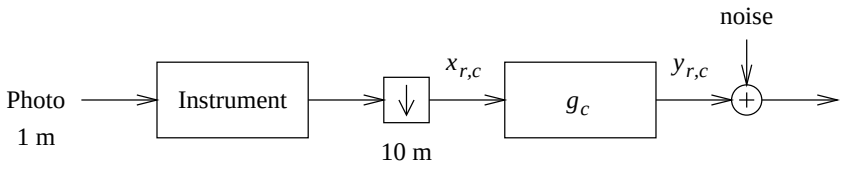

Figure 3. Simulated SPOT acquisition process.

The applied gains g_c^* (see Figure 4) were generated randomly using an uniform i.i.d. law on $[0.975\ ;\ 1.025]$, which corresponds to the order of magnitude of the gains estimated during calibration phases. Of course, no mirroring has been accounted for in the sampling of the gains.

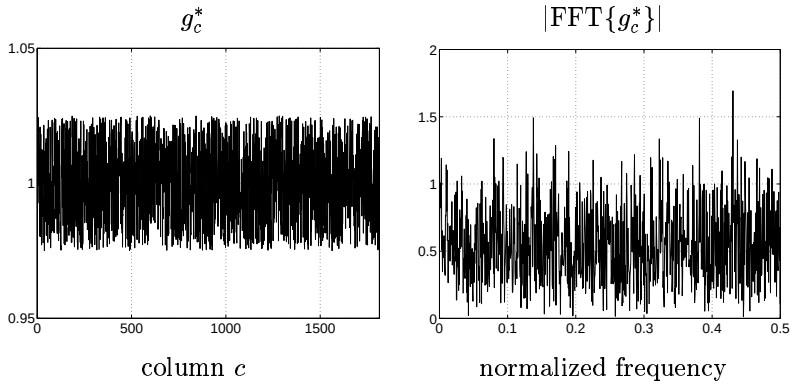

Figure 4. Spatial and frequential representation of the simulated gains g_c^*.

Two indices have been used to quantify the quality of the estimated gains:

$$\sigma_R = \sqrt{\frac{1}{C}\sum_{c=1}^{C}\left(\frac{\hat{g}_c}{g_c^*} - 1\right)^2}, \qquad \mathrm{max}_V = \max_c \left|\frac{\hat{g}_c}{g_c^*} - \frac{\hat{g}_{c+1}}{g_{c+1}^*}\right|,$$

namely, *normalized mean square error* σ_R and *visual maximum* $\max_V$. The interest of the latter is to provide the maximum calibration error between two neighboring columns.

4.2. EMPIRICAL ESTIMATES

The gains are very badly estimated with the empirical estimate $\widehat{g}_c^0$ ($\sigma_R = 9.6\%$ and $\max_V = 2.89\%$) as it is very sensitive to the observed landscape. Indeed, one can clearly see on Figure 5 that the mirroring effect performed on $\boldsymbol{x}$ is retrieved on the estimated gains.

When the image mean is computed locally, relatively good results can be obtained. We have computed $\widehat{g}_c^1$ with a rectangular window $w_k = 1/9, k = -4 \cdot 4$. The corresponding indices are $\sigma_R = 0.79\%$ and $\max_V = 2.19\%$, if columns near the boundaries of the image are discarded. One could still try to improve such a result, *e.g.* using other shapes than rectangular windows.

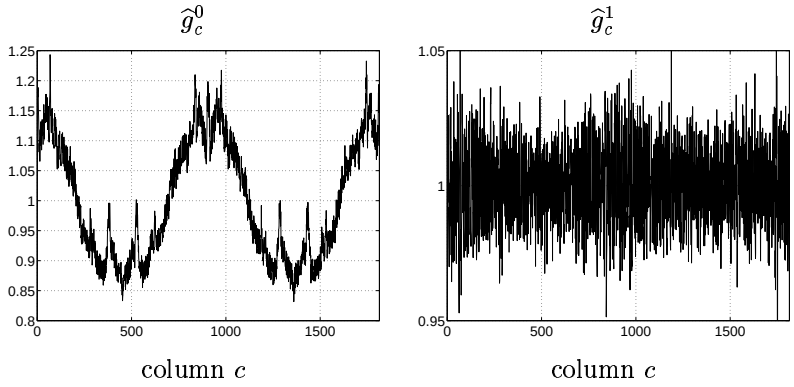

Figure 5. Spatial representation of the gains estimated empirically estimated with $\widehat{g}_c^0$ and $\widehat{g}_c^1$.

4.3. ML ESTIMATES

As seen in § 3.1, the ML estimate for the additive relation (2) is interesting to study as it leads to a set of $C-1$ univariate minimization problems. The minimizers have close-form expressions for $\phi(x) = x^2$ and $\phi(x) = |x|$ but not for $\phi_s(x) = \sqrt{s^2 + x^2}$ and $\phi_s(x) = \frac{x^2}{s^2+x^2}$.

Akin to the empirical estimation using $\widehat{g}_c^0$, the obtained results are very sensitive to the observed landscape. The very low frequencies of the gain (in the range [0 ; 0.05]) are overestimated (see Figure 6). One can try to filter out very low frequencies, although such a procedure is purely *ad hoc*. Performance of such filtered estimates are gathered in TABLE 1 for best values of the threshold parameter s in the last two cases. Low frequencies in the range [0 ; 0.05] have been cut, as depicted by Figure 6. Such results clearly show that edge-preserving models ($\phi(x) = \sqrt{s^2 + x^2}$ and $\phi(x) = \frac{x^2}{s^2+x^2}$)) outperform the two simpler alternatives.

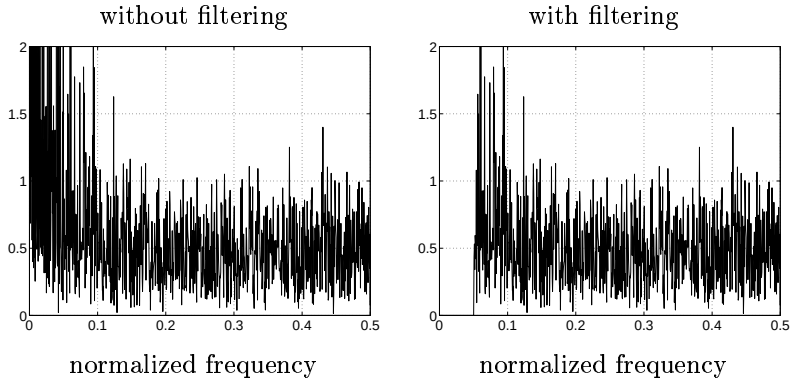

Figure 6. Frequential representation of the gains estimated with the ML estimate, with $\phi(x) = x^2$, in the additive case.

$\phi(x)$	s	σ_R	$\max_V$
x^2		0.75%	1.85%
$\lvert x \rvert$		0.72%	2.70%
$\sqrt{s^2+x^2}$	0.01	0.53%	0.90%
$\frac{x^2}{s^2+x^2}$	0.05	0.49%	0.68%

TABLE 1. Performance of filtered ML estimate for the additive case.

Since only univariate criteria (10) have to be minimized in the additive ML case, one can easily study the unimodality of such criteria, even in the non convex case of $\phi_s(x) = \frac{x^2}{s^2+x^2}$. Figure 7 depicts one such criterion for three different values of parameter s. For $s = 0.05$, which gave the better results, the criterion is unimodal. For large values of s (*e.g.*, $s = 0.5$), the criterion is even near to quadraticity. For small values of s (*e.g.*, $s = 0.01$) local minima appear. The shape of $J^l_{ML}(\delta g) = \sum_r \phi(\delta g - \delta y_r)$ can be studied more precisely using an asymptotic viewpoint: if we assume that δy_r are all samples from a random variable δY, then we can expect that the basic asymptotic statistical result

$$\forall \delta g, \quad \lim_{R\to\infty} \frac{1}{R} \sum_r \phi(\delta g - \delta y_r) = \mathrm{E}_{\delta Y}[\phi(\delta g - \delta Y)]$$

almost surely. Let us also assume that the probability law of δY admits a density $f_{\delta Y}$:

$$\mathrm{E}_{\delta Y}[\phi(\delta g - \delta Y)] = \int_u \phi(\delta g - u) f_{\delta Y}(u) du = (\phi \star f_{\delta Y})(\delta g).$$

Hence, J^l_{ML} converges to a smoothed version of $f_{\delta Y}$ for a sufficiently high number of processed rows. Since $f_{\delta Y}$ can be expected to be a nicely unimodal function, J^l_{ML}

will tend to a unimodal criterion provided that ϕ is unimodal. In the finite data case, since we have $J^l_{ML} = \phi \star \sum_r \delta_{\delta y_r}$ if δ_u denotes the shifted Dirac distribution around u, unimodality of J^l_{ML} can be reached if ϕ is smooth enough, even if it is not convex.

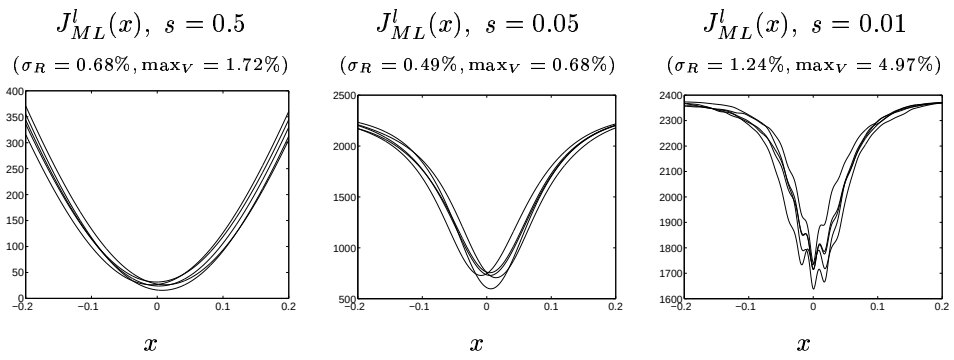

Figure 7. Representation of $J^l_{ML}(\delta g^l_c) = \sum_r \phi(\delta g^l_c - \delta y^l_{rc})$ with $\phi_s(x) = \frac{x^2}{s^2+x^2}$ for 5 different columns and various values of s.

We do not report ML estimation results for the multiplicative relation (1), since they also tend to overestimate low frequencies of the gain sequence, while this case does not benefit from the same structural simplicity as the additive counterpart.

4.4. MAP ESTIMATES

In the case of MAP estimation, neither the additive nor the multiplicative relations yield a separable criterion. However, the additive relation (2) still provides a simpler estimation structure. Firstly, no approximation is required to obtain quadratic or half-quadratic criteria. Secondly, there is one hyperparameter less in the additive structure, since T and σ_g^2 only intervene through the ratio T/σ_g^2 (in the following, we have chosen $T = 1$). Finally, we have found experimentally that results obtained for the multiplicative relation are not as good as for the additive one, so we will not comment on them hereafter.

TABLE 2 gathers the best results (with respect to s and σ_g^2) obtained for different functions ϕ. Such results were obtained without any post-filtering operation, contrarily to ML estimation. Once again, edge-preserving functions provide significantly better results, and the non convex behaviour of $\phi(x) = \frac{x^2}{s^2+x^2}$ reveals preferable to any other choices.

It is interesting to study the frequency representation of the estimated gains with respect to the parameter σ_g^2. The resulting spectrum is plotted on Figure 8 for $\phi(x) = \frac{x^2}{s^2+x^2}$ with $s = 0.05$, for three contrasted values of σ_g^2. As expected, for large values of σ_g^2, MAP estimation becomes equivalent to ML estimation and leads to overestimated very low frequency components. For values of σ_g^2 around the optimum tuning, it appears that low frequency components are slightly un-

ϕ	s	σ_g^2	σ_R	$\max_V$
x^2		$8e^{-4}$	0.63%	1.54%
$\sqrt{s^2+x^2}$	0.01	$3e^{-4}$	0.49%	0.88%
$\frac{x^2}{s^2+x^2}$	0.05	$5e^{-5}$	0.43%	0.50%

TABLE 2. Results obtained with the MAP estimator for the additive relation.

derestimated. At very low frequencies, it is very difficult to separate between the contributions from the gains and from the landscape.

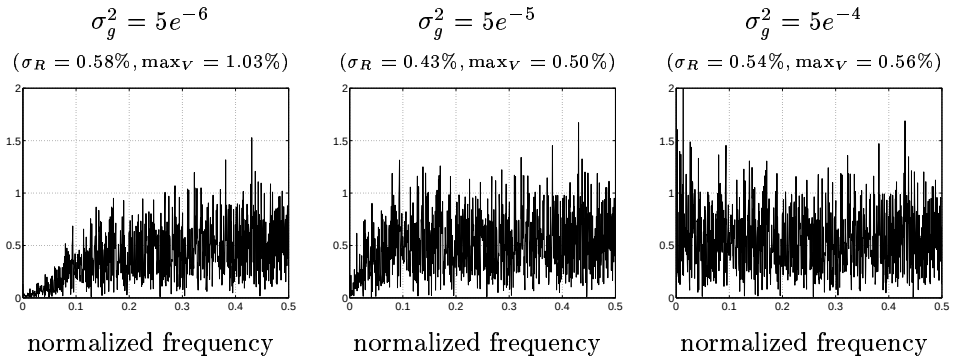

Figure 8. Frequency representation of the gains estimated using MAP in the additive case, for three values of σ_g^2 ($T = 1$).

5. Conclusions and perspectives

Imperfect detectors in a CCD linear array generate a stripe effect when the array is used to scan images. This is a non negligible source of degradation in SPOT satellite imaging system. Accurate estimation of each detector response is required in order to compensate for the imperfections. In the present paper, a statistical self-calibration method has been proposed to perform linear correction. Self-calibration means that no specific training data is required, in contrast with current procedures that involve periodical calibration phases.

Our approach is based on a statistical spatial model for the observed image. The best results are obtained with a Markov model for the logarithm of pixel intensities, associated to a non convex energy, when a posterior likelihood is maximized with respect to the logarithm of detector gains. The corresponding prior is a simple i.i.d. centered Gaussian law.

We are presently extending our contribution to a generalized non-linear model for the detectors response. It makes the detectors response g_c depend on the current

pixel intensity x_{rc}, according to the following three parameter model:

$$g_c(x_{rc}) = (\alpha_c - \beta_c e^{-\tau_c x_{rc}}) x_{rc},\ \alpha_c \approx 1,\ \beta_c \approx 0,\ \tau_c > 0.$$

Ackowledgement

The first two authors would like to thanks the CNES to its support on this study and S. LESAGE and O. ANTOINE for their help for simulations.

References

1. S. Geman and D. McClure, "Statistical methods for tomographic image reconstruction," in *Proceedings of the 46th Session of the ISI, Bulletin of the ISI*, vol. 52, pp. 5–21, 1987.
2. P. Charbonnier, L. Blanc-Féraud, G. Aubert, and M. Barlaud, "Two deterministic half-quadratic regularization algorithms for computed imaging," in *Proceedings of the International Conference on Image Processing*, vol. 2, pp. 168–172, 1994.
3. D. Geman and G. Reynolds, "Constrained restoration and recovery of discontinuities," *IEEE Transactions on Pattern Analysis and Machine Intelligence*, **PAMI-14**, pp. 367–383, mars 1992.
4. J. Idier, "Convex half-quadratic criteria and interacting auxiliary variables for image restoration," rapport technique, GPI–LSS, 1999.
5. A. H. Delaney and Y. Bresler, "Globally convergent edge-preserving regularized reconstruction: an application to limited-angle tomography," *IEEE Transactions on Image Processing*, **IP-7**, pp. 204–221, février 1998.